Desalination and Water Treatment
www.deswater.com

doi: 10.1080/19443994.2016.1143880

57 (2016) 24913–24924
November

OFFIS: a method for the assessment of first flush occurrence probability in storm drain inlets

Andres Torres, Camilo Alberto Salamanca-López, Sebastián Felipe Prieto-Parra, Sandra Galarza-Molina*

Grupo de Investigación Ciencia e Ingeniería del Agua y el Ambiente, Facultad de Ingeniería, Pontificia Universidad Javeriana, Carrera 7 # 40 – 62, sede Bogotá, Colombia, Tel. +57 1 3208320, ext. 5553; emails: andres.torres@javeriana.edu.co (A. Torres), csalamanca05@hotmail.com (C.A. Salamanca-López), prieto.s@javeriana.edu.co (S.F. Prieto-Parra), salogamo@gmail.com (S. Galarza-Molina)

Received 9 July 2015; Accepted 12 January 2016

ABSTRACT

First flush analysis entails the comparison of pollutographs and hydrographs. The difficulty of this type of analysis also lies in the fact that it runs up against a wide array of experimental uncertainties associated with the collection of temporal data. The present paper proposes a methodology that accounts for the aforementioned factors in the calculation of occurrence probability for first flush as measured at a storm drain inlet. Considering concepts such as standard uncertainty (for first flush uncertainties), the Monte Carlo method, the Spearman correlation rank test and Partial Least Squares Regressions (for analysis of the relationship between precipitation characteristics and first flush). This methodology has been coined "Occurrence probability of First Flush In Storm drain inlets" (OFFIS). Developed in R, OFFIS detected first flush in a specific case study.

Keywords: First flush; Stormwater pollution; Total suspended solids; Urban runoff; PLS

1. Introduction

Runoff passing through urbanized areas exhibits higher levels of pollution, a situation best understood in light of the fact that it washes over the surface, picking up accumulated pollutants (e.g. urban roads TSS varied between 11 and 5,400 mg/L—Event Mean Concentrations [1]) [2]. First flush, the greatest mass of pollutants contained in a small fraction of volume, is a phenomenon that stems from initial precipitation. Rain-event pollutant loads associated with this phenomenon may be higher than ones associated with dry weather period wastewater [3,4].

It is recommended to consider five factors when discussing the relationship between total suspended solids (TSS) and first flush. Bertrand-Krajewski [5] and Li et al. [6] found that TSS concentrations correlate to event intensities. Li et al. [7] show that the Antecedent Dry Weather Period (ADWP) also affects ($R^2 = 0.95$, p-value < 0.01) pollutant fluctuations in urban runoff. Moreover, maximum rainfall intensity, time to peak [8], and impervious area percentage [9,10] play a role in the TSS load present in first flush.

Seeing as first flush is a site-specific phenomenon [8,10–13] with strong variations from one storm event to another [14], a universal set of climate, rainfall, and runoff characteristics or universal types of regression curve cannot be applied [8]. It then becomes necessary

*Corresponding author.

to frame the issue in terms of the occurrence probability of first flush. Owing to two distinct obstacles that go hand-in-hand with the study of the first flush phenomenon as observed during a rain event: (i) it is cumbersome to obtain pollutographs corresponding to hydrographs in temporal terms; (ii) myriad experimental uncertainties accompany the acquisition of temporal data.

Hence, the present study establishes a methodology to determine the occurrence probability of first flush in a storm drain inlet and not just first flush itself. We define the occurrence probability of first flush in a storm drain inlet as the probability that has a rainfall event of falling within first flush zones in line with Bertrand-Krajewski et al. [14]. To assess the probability and importance of the first flush effect for each storm event, we determine the uncertainties related to first flush measurement.

In order to apply the proposed methodology, we observed during rainfall events a storm drain inlet. The inlet is located on a highly transited Avenue in Bogota. As well, the methodology employs basic data-acquisition tools (e.g. ruler and chronometer). In the same vein, first flush is analyzed through the lens of a rainfall event's specificities in order to identify patterns between pollutant loads and precipitation characteristics.

2. Materials and methods

A five-stage procedure is put forth to assess first flush occurrence probability during rainfall events in a storm drain inlet (see Fig. 1). We developed a script in R coding [15] called "OFFIS," which stands for the Occurrence probability of First Flush In Storm drain inlets.

First, is necessary to measure the inflows (Q) and the water quality (e.g. TSS, turbidity) in the drain inlet chosen (Step 1 Fig. 1). For the above, we define the quality parameters to measure and the maximum number of water samples per event (X). To measure Q, we employed basic data acquisition tools (e.g. ruler and chronometer).

Second, in order to have the M(V) curve (dimensionless curves of cumulative pollutant mass versus cumulative discharged volume [14]) per event (Step 2 Fig. 1) we calculate the inflow (Q) and the quality parameters concentrations. The latter are determined in accordance with procedures established by the Standard Methods [16]. Then, to tackle the uncertainties associated with first flush we appraise the standard uncertainty (e.g. ISO [17]; ISO [18]) of M(V) curves and field measurements (TSS and Q). The uncertainty $u(y)$ of a value y depends on other values with a function $y = f(x_1, x_2, \ldots, x_N)$, known as "composed standard uncertainty" [17]. This value results from the law of uncertainty propagation, whereby if estimated covariance between x_i and x_j is zero, the law can be simplified such that Eq. (1) [19]:

$$u^2(y) = \sum_{i=1}^{N} \left(\frac{\partial f}{\partial x_i}\right)^2 u^2(x_i) \tag{1}$$

The composed standard uncertainty of TSS concentration, flow rate Q, normalized total mass M, and volume V (u(TSS), $u(Q)$, $u(M)$, $u(V)$) are computed following Eq. (1). Therefore, Equations Eqs. (2)–(5) are proposed:

$$u(\mathrm{TSS}) = \sqrt{\frac{1}{v^2}u^2(m_\mathrm{f}) + \frac{1}{v^2}u^2(m_\mathrm{o}) + \frac{u^2(v)}{v^4}(m_\mathrm{f} - m_\mathrm{o})^2} \tag{2}$$

$$u(Q) = \frac{1}{u^2(\Delta t)}\sqrt{(w\,\Delta h)^2 u^2(l) + (l\,\Delta h)^2 u^2(w) + (wl)^2 u^2(\Delta h) + \left(\frac{wl\,\Delta h}{\Delta t}\right)^2 u^2(\Delta t)} \tag{3}$$

$$u(M) = 100\sqrt{(Q\,\Delta t)^2\, u^2(\mathrm{TSS}) + (\mathrm{TSS}\,\Delta t)^2\, u^2(Q) + (\mathrm{TSS}\,Q)^2\, u^2(\Delta t)} \tag{4}$$

$$u(V) = 100\sqrt{(w\,\Delta h)^2\, u^2(l) + (l\,\Delta h)^2\, u^2(w) + (wl)^2\, u^2(\Delta h)} \tag{5}$$

For u(TSS), m_o is the dry filter weight (TSS laboratory test), m_f the sum of m_o, and TSS weight retained by the filter paper, v the sample water volume used for TSS concentration. For $u(Q)$, w is the

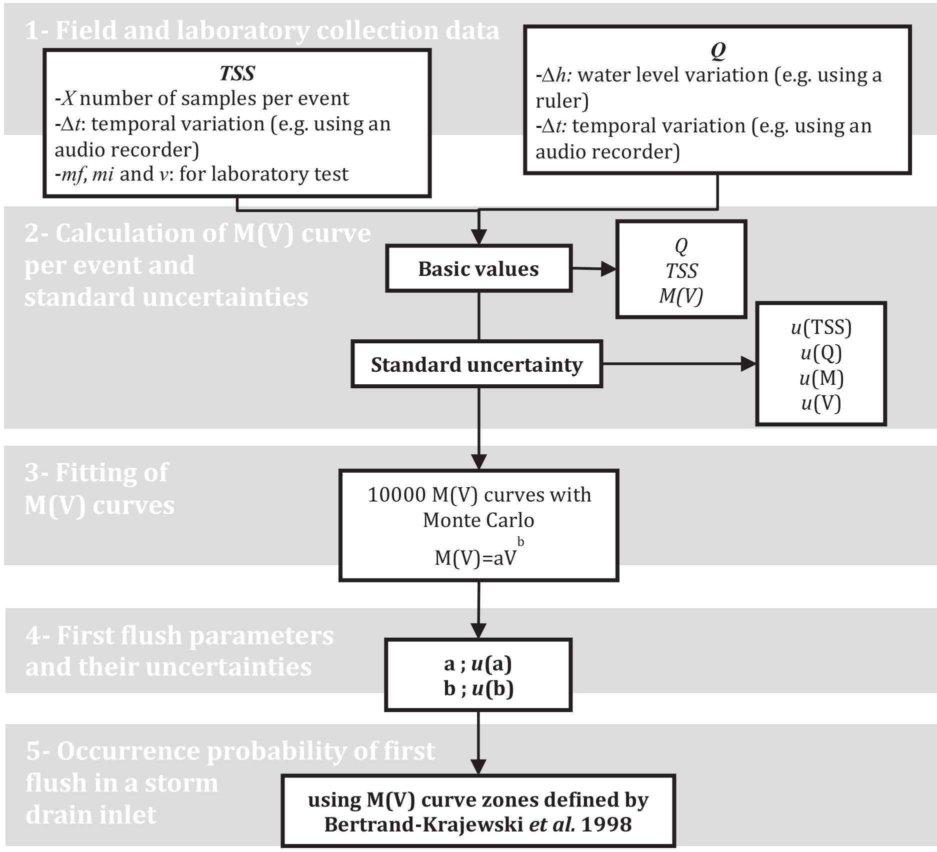

Fig. 1. OFFIS methodology procedure.

Fig. 2. Case study site location: storm drain inlet in the 39th Street (4°37′37.66′′N–74°4′0.50′′O). (Adapted: Map data © 2015 Google [27]).

average width of the storm drain inlet, l the average length of the storm drain inlet, Δh the water level variation, Δt the temporal variation between consecutive water level measurements, and Q the flow rate. The standard uncertainties $u(m_f$ or $m_o)$ and $u(v)$, associated with the measurement of mass and volume, are equal to the half of instruments precision used for measurements with 95% confidence. This assumption can be done considering that the measurements of mass and volume with respective devices (e.g. mass balance, ruler) follow a normal distribution.

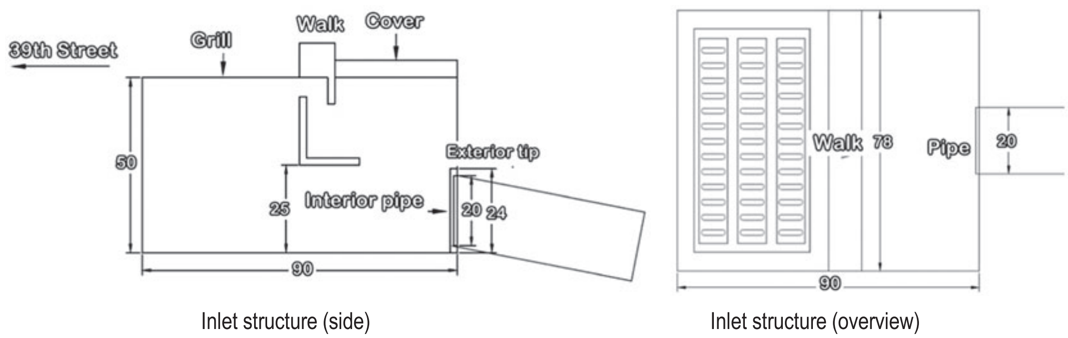

Fig. 3. Inlet structure geometry (centimeters).

Table 1
Summary of pollutograph, hydrograph, hydrological characteristics, and *a* and *b* parameters for each event. TSS_{max} and TSS_m in mg/l, Q_{max} in l/min, V_{tot} in liters, M_{tot} in kg, ADWP and *D* in h, *P* in mm, I_m, and I_{max} in mm/h. In italics are the events that are in Fig. 4

Event	Date	TSS_{max}	TSS_m	Q_{max}	V_{tot}	M_{tot}	ADWP	P	I_m	I_{max}	D	a	b
1	4/10	1,140	439	334	1,932.3	0.7	251.50	0.80	1.20	3.60	0.67	21.79	0.33
2	4/10	2,150	1,044	1,053	68,891.6	49.0	0.83	18.80	16.11	34.80	1.42	4.09	0.70
3	6/10	525	254	32	926.1	0.2	4.50	3.50	1.75	5.40	1.80	4.99	0.65
4	*11/10*	*905*	*441*	*32*	*744.1*	*0.4*	*7.83*	*3.50*	*2.63*	*6.60*	*1.17*	*1.31*	*0.96*
5	12/10	3,150	1,500	1,053	28,775.7	45.3	6.60	6.60	4.40	16.20	1.33	1.98	0.86
6	8/11	330	110	18	158.5	0.0	40.12	2.55	5.08	7.62	0.50	1.59	0.92
7	*10/11*	*1,760*	*555*	*155*	*1,932.6*	*1.1*	*21.00*	*7.00*	*10.50*	*25.80*	*0.67*	*4.95*	*0.65*
8	*10/11*	*820*	*4,157*	*1,053*	*7,073.4*	*4.6*	*2.00*	*18.00*	*13.50*	*46.80*	*1.17*	*0.68*	*1.09*

Third, using the Monte Carlo method we produce a large number of possible M(V) curves for each storm event (Step 3 Fig. 1)—e.g. 10,000 total runs—. Monte Carlo is a numeric method used for uncertainty evaluation [20–22]. As an example, in 2011, Sharifi et al. [23] developed a model based on traditional first flush formulations and Monte Carlo method. They evaluated the impact of incorporate first flush uncertainties in the first flush design concept for Best Management Practices Systems (BMPs). This methodology allows optimizing the BMP design using the probability of exceeding load-based criteria instead of a concentration based criteria.

For all simulations/events, parameters *a* and *b* were fitted using equation $M = aV^b$ proposed according to Bertrand-Krajewski et al. [14] (based on 197 rainfall events for six catchments). With these possible M(V) curves we estimate the uncertainties associated with first flush parameters (Step 4 Fig. 1) reached *via* equations Eqs. (2)–(5).

Finally, we computed the occurrence probability of first flush in a storm drain inlet (Step 5 Fig. 1) classifying the rainfall event probabilities of being within specific first flush zones. We used the typology of M(V) curves proposed by Bertrand-Krajewski et al. [14].

Additionally to the proposed methodology, the relation between both *a* and *b* parameters with rainfall characteristics are explored. We use Spearman rank correlation test and linear and PLS (Partial Least Squares Regressions) models for both *a* and *b* . The linear and PLS models can be constructed for both *a* and *b* (each a dependent variable *Y*) given rainfall characteristics (explanatory variables) that form the *X* matrix.

Table 2
Uncertainties of instruments and storm drain inlet dimensions

Source	Notation	Magnitude	Unit
Beaker	$u(v)$	0.25	ml
Chronometer	$u(\Delta t)$	0.50	s
Mass balance	$u(m)$	0.05	mg
Drain inlet—width	$u(w)$	0.58	cm
Drain inlet—length	$u(l)$	0.50	cm
Ruler	$u(\Delta h)$	0.50	cm

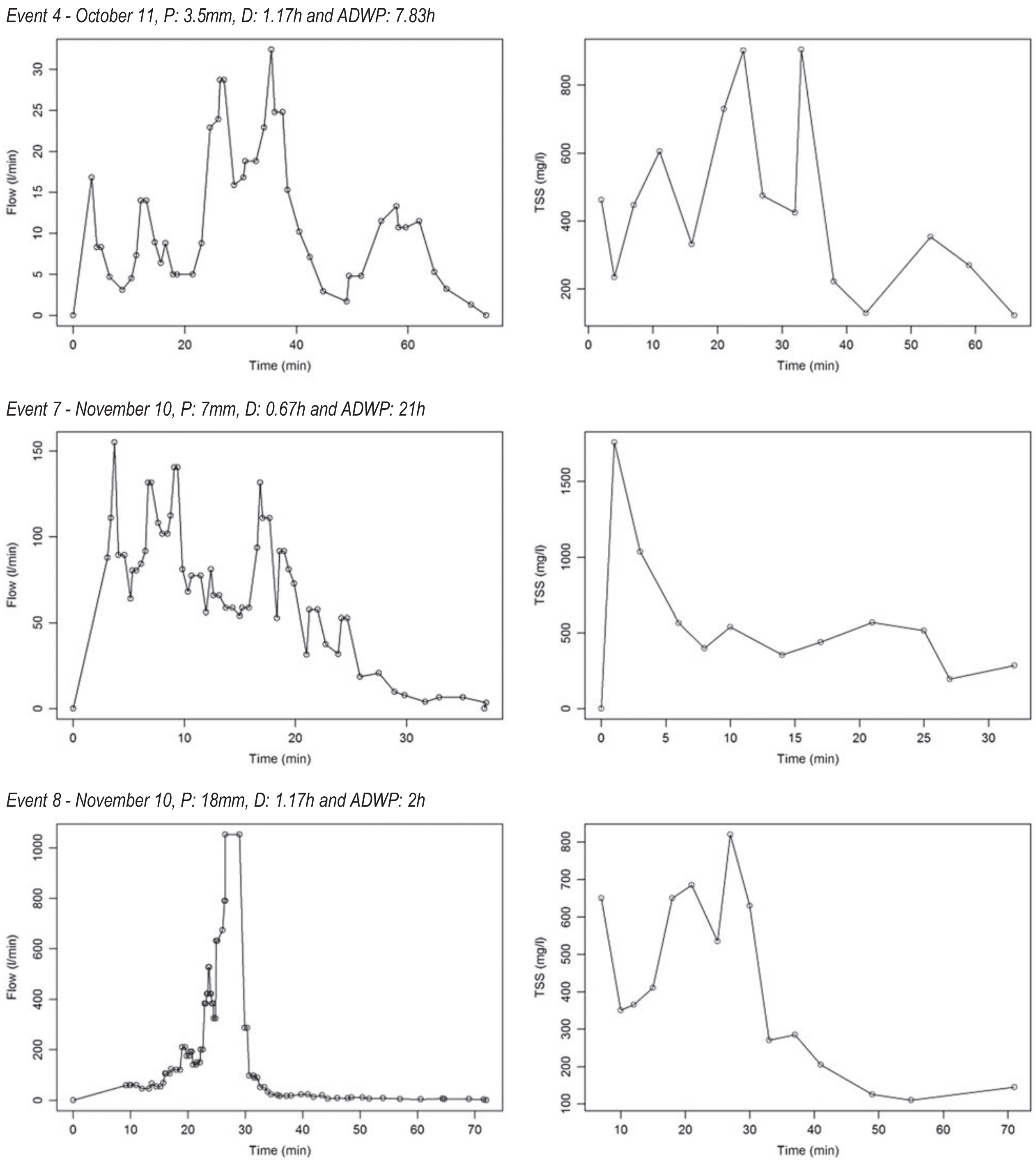

Fig. 4. Hydrographs (left) and pollutographs (right) for events of 11 October and 10 November (see Table 2) (P: precipitation, D: event duration and ADWP: Antecedent Dry Weather Period).

This last step is carried out using the PLS library [24]. Linear and PLS regression models with β coefficients for each variable can be obtained, allowing for the prediction Y_{sim} of further Y values (Eq. (6)). Each of the 10,000 fitted linear models—along with adjustment quality, residual normality, and β coefficients per Eq. (6)—can be assessed [25]. The coefficients laid out in facilitate the establishment of relevance for every X variable (X_1, X_2, …, X_n) compared to the dependent variable Y (a or b in this case) [26].

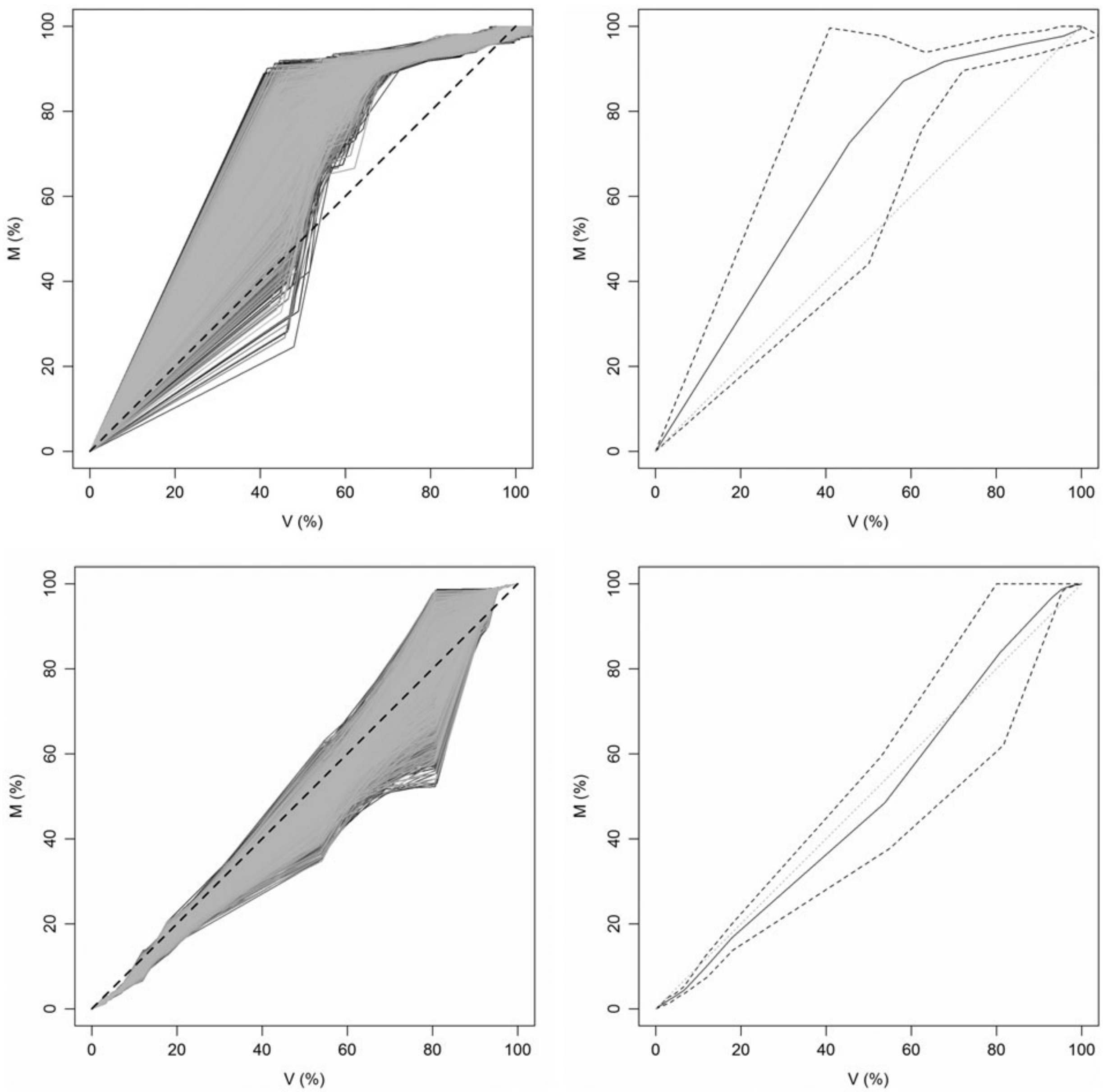

Fig. 5. 10,000 Monte Carlo simulated M(V) curves (left) for events 1 (4 October, P: 0.8 mm, D: 0.67 h and ADWP: 251 h) and 8 (10 November, P: 18 mm, D: 1.17 h and ADWP: 2 h); most probable M(V) curves with upper and lower uncertainty boundaries (right).

$$Y_{\mathrm{sim}} = \beta_0 + \beta_1 X_1 + \beta_2 X_2 + \ldots + \beta_n X_n \quad (6)$$

In order to know which are the hydrological variables most relevant to a and b parameters, we compute the absolute values of the weighting factors (β_1–β_n, Eq. (6)) of the PLS models for both parameters. This procedure quantifies the effect of each hydrological variable on first flush, from Position 1 (most important) to 5 (least important). Undertaken for each of the 10,000 PLS models fitted, this step is combined with a recurrence indicator (RI) to reveal the number of times (1–10,000) that a certain hydrological variable occupies the same position; subsequently, this number is divided by the total number of simulations (10,000).

For illustrative purposes, we applied OFFIS to a case study as spelled out below. A storm drain inlet at the intersection of 39th Street and 7th Avenue (Bogota, Colombia), on the northeastern side of the street

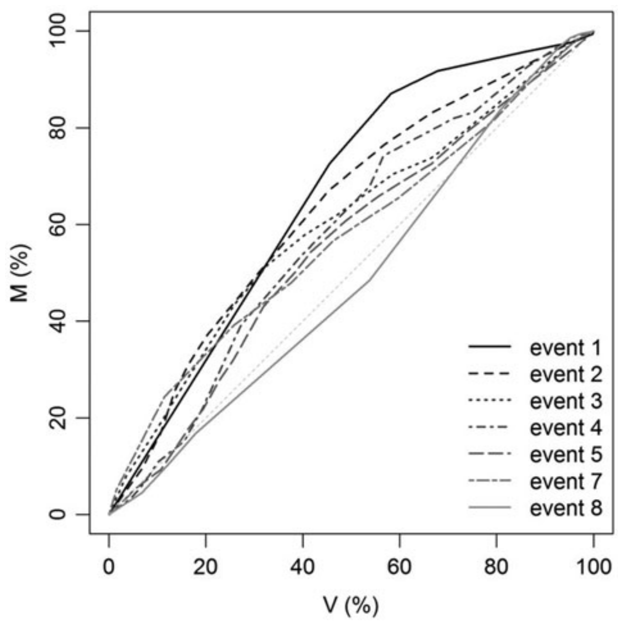

Fig. 6. Most representative M(V) curves, which correspond to the second quartile for each rain event (except for Event Six).

(coordinates 4°37′37.66′′N 74°4′0.50′′W; see Fig. 2), serves as the case study site. The storm inlet is located in a commercial/residential area, with a drainage area of 230 m^2 (100% impervious) and a slope of 2.8%.

Flow measurements done at the storm drain inlet used relied on a tank with entrance and exit flows (Fig. 3). We estimate the incoming water volume by closing the outgoing pipe with a custom-made waterproof cap; the temporal variation of storage volume is figured using water surface-level variations (Δh) (Step 1 Fig. 1).

In order to characterize rainwater runoff we collected 15 samples per event. The turbidity and TSS concentrations were determined at the Pontificia Universidad Javeriana's (PUJ) water quality laboratory in accordance with procedures established by the Standard Methods (2540D—TSS dried at 103–105°C and 2130B—Nephelometric method) [16].

Hydrographs and pollutographs are obtained for eight precipitation events between October (4th, 6th, 11th, 12th) and November (8th, 10th) of 2011. To arrive at the hydrological characteristics of each storm event, high frequency registers (10-min time steps) were stationed at a rain gauge 400 meters from the experimental site. The following values were established for each event: ADWP, rainfall depth P, average

Table 4
Spearman correlation (ρ) for hydrological characteristics of hydrographs and pollutographs

	TSS_{max}	TSS_m	Q_{max}	V_{tot}	M_{tot}
TSS_{max}	1.00	0.98	0.73	0.79	0.83
TSS_m	0.98	1.00	0.68	0.74	0.81
Q_{max}	0.73	0.68	1.00	0.93	0.95
V_{tot}	0.79	0.74	0.93	1.00	0.98
M_{tot}	0.83	0.81	0.95	0.98	1.00
ADWP	−0.19	−0.26	−0.51	−0.62	−0.57
P	0.46	0.52	0.65	0.78	0.78
I_m	0.21	0.26	0.44	0.55	0.57
I_{max}	0.29	0.33	0.59	0.64	0.67
D	0.27	0.31	0.33	0.47	0.39

Table 5
Spearman correlation test p-values (Table 4)

	TSS_{max}	TSS_m	Q_{max}	V_{tot}	M_{tot}
TSS_{max}	–	<0.01	0.04	0.03	0.02
TSS_m	<0.01	–	0.06	0.05	0.02
Q_{max}	0.04	0.06	–	<0.01	<0.01
V_{tot}	0.03	0.05	<0.01	–	<0.01
M_{tot}	0.02	0.02	<0.01	<0.01	–
ADWP	0.66	0.54	0.19	0.11	0.15
P	0.26	0.19	0.08	0.02	0.02
I_m	0.62	0.54	0.28	0.17	0.15
I_{max}	0.50	0.43	0.13	0.10	0.08
D	0.53	0.45	0.42	0.24	0.35

Table 3
Distribution probabilities for M(V) curve zones defined by Bertrand-Krajewski et al. [14] (event six omitted)

b value		Zone	Space between M(V) curve and bisector		EV1	EV2	EV3	EV4	EV5	EV7	EV8
$b < 1$	$0 < b \leq 0.185$	1	Positive space	High	4.8	0.0	0.0	0.0	0.0	0.0	0.0
	$0.185 < b \leq 0.862$	2		Medium	95.2	100	100	92.2	90.8	100	0.0
	$0.862 < b \leq 1.000$	3		Insignificant	0.0	0.0	0.0	7.8	9.2	0.0	0.7
$b > 1$	$1.000 < b \leq 1.159$	4	Negative space	Insignificant	0.0	0.0	0.0	0.0	0.0	0.0	78.4
	$1.156 < b \leq 5.395$	5		Medium	0.0	0.0	0.0	0.0	0.0	0.0	20.9
	$5.395 < b < \infty$	6		High	0.0	0.0	0.0	0.0	0.0	0.0	0.0

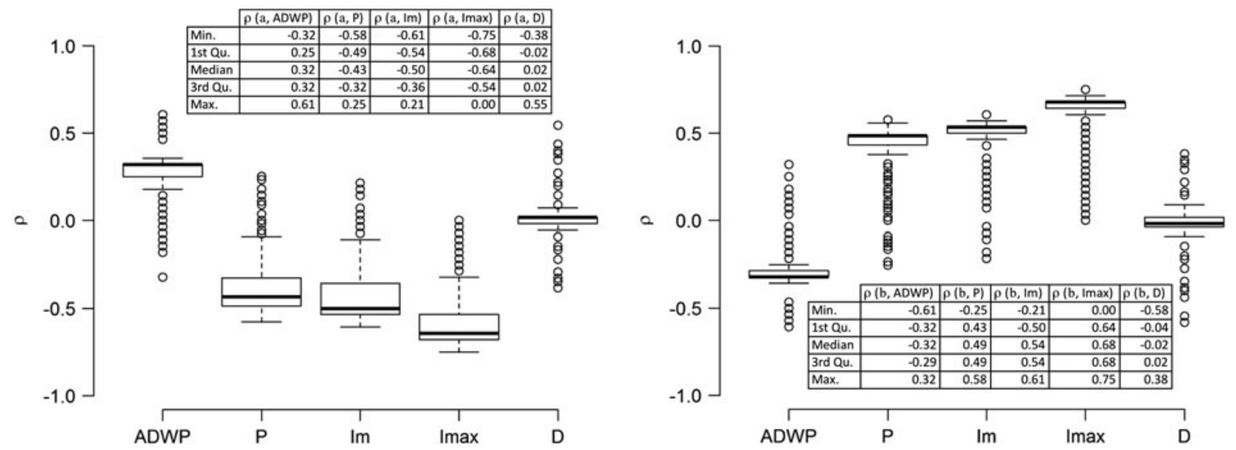

	ρ (a, ADWP)	ρ (a, P)	ρ (a, Im)	ρ (a, Imax)	ρ (a, D)
Min.	-0.32	-0.58	-0.61	-0.75	-0.38
1st Qu.	0.25	-0.49	-0.54	-0.68	-0.02
Median	0.32	-0.43	-0.50	-0.64	0.02
3rd Qu.	0.32	-0.32	-0.36	-0.54	0.02
Max.	0.61	0.25	0.21	0.00	0.55

	ρ (b, ADWP)	ρ (b, P)	ρ (b, Im)	ρ (b, Imax)	ρ (b, D)
Min.	-0.61	-0.25	-0.21	0.00	-0.58
1st Qu.	-0.32	0.43	-0.50	0.64	-0.04
Median	-0.32	0.49	0.54	0.68	-0.02
3rd Qu.	-0.29	0.49	0.54	0.68	0.02
Max.	0.32	0.58	0.61	0.75	0.38

Fig. 7. Spearman correlation coefficient (ρ) between a (left) and b (right), M(V) fitting parameters and rainfall characteristics (ADWP, rainfall depth P, average intensity I_m, maximum intensity I_{max} and event duration D).

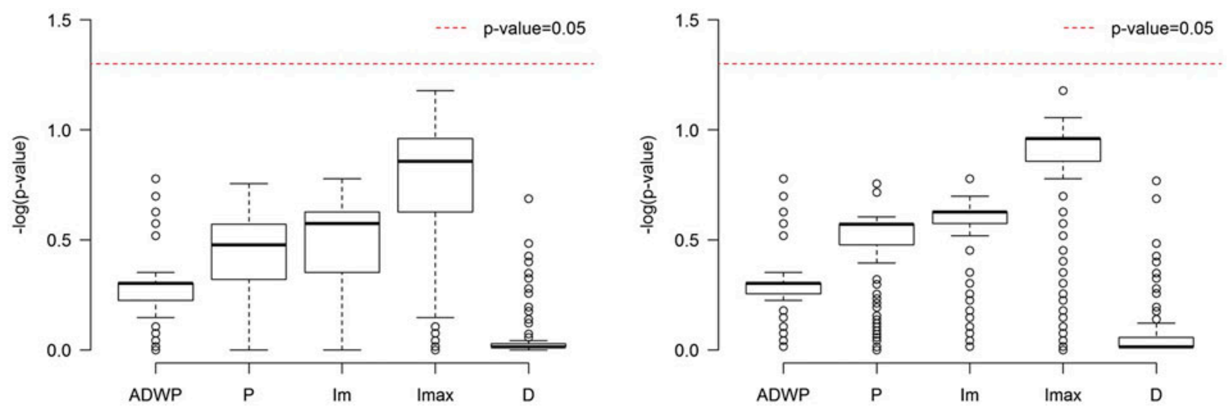

Fig. 8. p-values for Spearman correlation test between a (left) and b (right), M(V) fitting parameters and rainfall characteristics (ADWP, rainfall depth P, average intensity I_m, maximum intensity I_{max}, and event duration D).

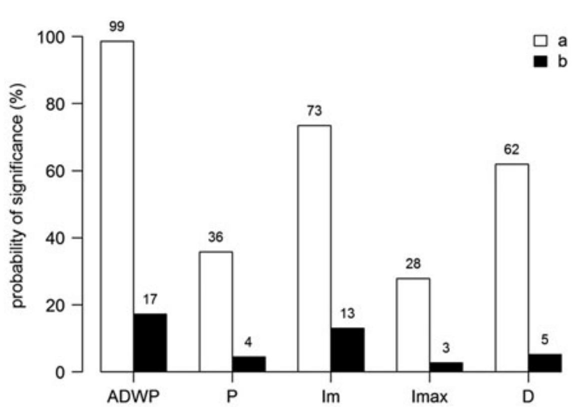

Fig. 9. Significance probability of coefficients from 10,000 linear models between a and b parameters and rainfall characteristics (ADWP, rainfall depth P, average intensity I_m, maximum intensity I_{max}, and event duration D).

intensity I_m, maximum intensity I_{max}, and event duration D (Step 1 Fig. 1).

3. Results and discussion

For the case study mentioned in the previous section, Table 1 summarizes hydrological and a and b parameters associated with each event (Step 2 Fig. 1), while Fig. 4 shows hydrographs and pollutographs for three rain events. This table also displays medium and maximum TSS concentrations for each event (TSS_m and TSS_{max}, respectively), with values ranging from 110 to 1,500 mg/l (TSS_m) and from 330 to 3,150 mg/l (TSS_{max}). These results are consistent with runoff TSS concentrations detected by other studies: 49–498 mg/l for the "Le Marais" catchment in Paris, France [28]; 15–377 mg/l for the Villa Cambiaso catchment in

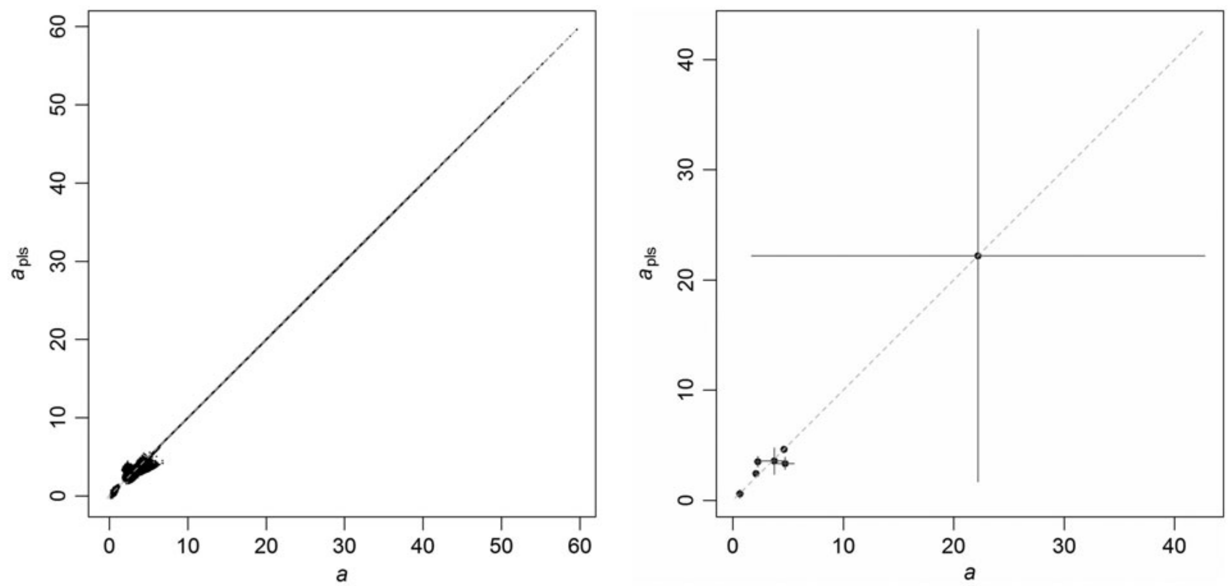

Fig. 10. Relationship between simulated a parameter (labeled a_{pls}) and observed a parameter (labeled a), r = 0.9926; r^2 = 0.9852, RMSE = 0.8091.

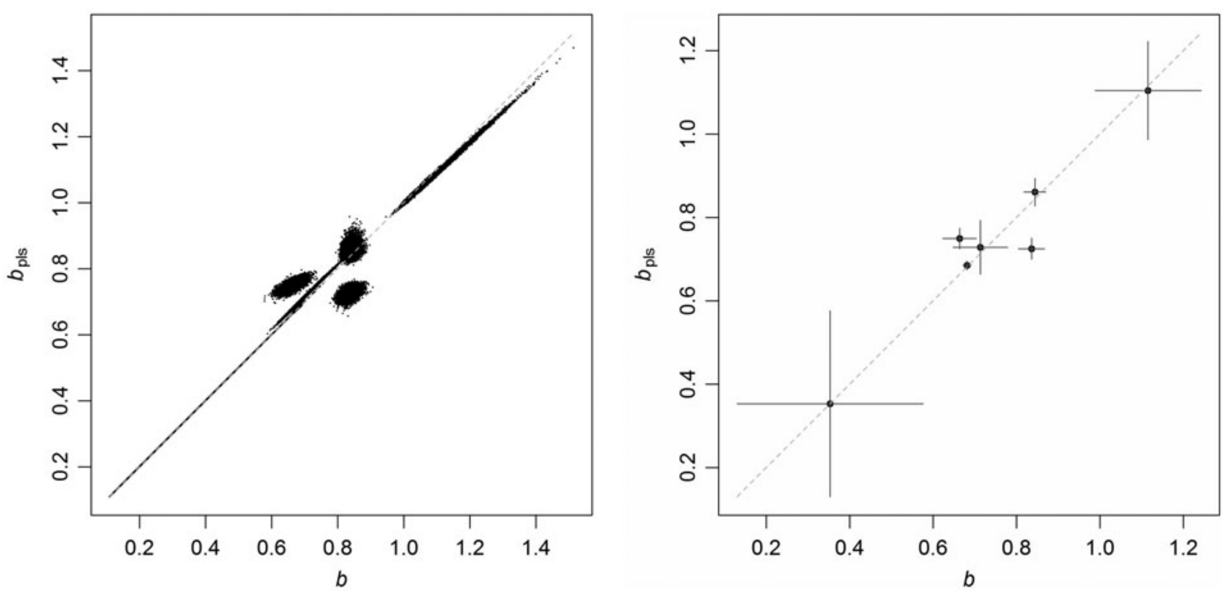

Fig. 11. Relationship between simulated b parameter (labeled b_{pls}) and observed b parameter (labeled b), r = 0.9490; r^2 = 0.9007, RMSE = 0.0649.

Genoa, Italy [29]; 120–1,400 mg/l for Zhengzhou City, China [2].

In Table 2 we summarized the precision of all instruments used for measurements, expressed as standard uncertainties (Step 2 Fig. 1).

M(V) curves are shown in Figs. 5 and 6 (Step 3 Fig. 1). On the left side of Fig. 4, 10,000 M(V) curve simulations for two events are depicted. Event Six is excluded from this analysis because data could not be properly adjusted to the M(V) function. Fig. 5's upper and lower boundaries (right side) represent the region encompassing 95% of the M(V) curves, a calculation done with quartiles, for there is no evidence that the data follow a normal distribution. The quartile calculation looks like: $[Q_1 - 1.5\ \text{IQR}, Q_3 + 1.5\ \text{IQR}]$, where Q_1 is the first quartile, Q_3 the

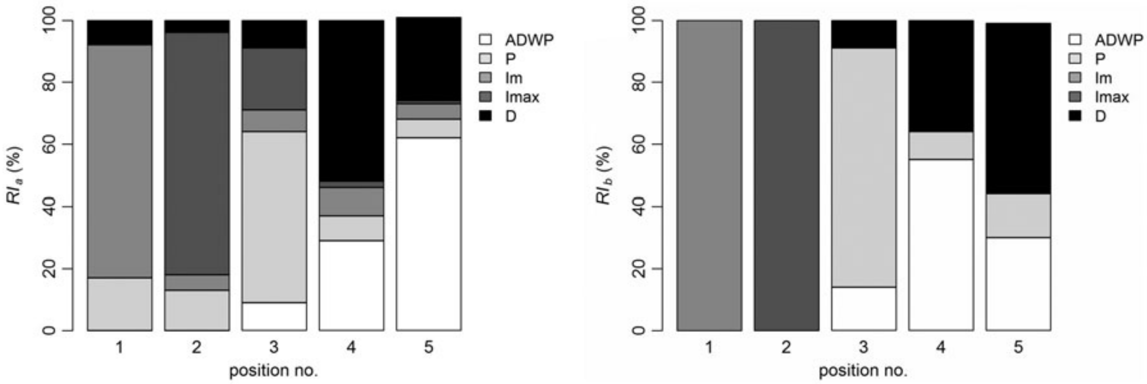

Fig. 12. Relevance indicator (RI) for a (left) and b (right) PLS models for ADWP, rainfall depth P, average intensity I_m, maximum intensity I_{max}, and event duration D.

third, and IQR the inter-quartile range [difference between Q_3 and Q_1] [30]. From Fig. 5, high M(V) curve variation and first flush are presented (Step 4 Fig. 1). Fig. 6 shows the most representative M(V) curves (Step 4 Fig. 1), which correspond to the second quartile for each rain event, with exception of event 6.

In Table 3 we show the occurrence probability of first flush in our case study for each event (Step 5 Fig. 1). We classified probabilities of being within specific first flush zones for each event, in line with Bertrand-Krajewski et al. [14]. Six of the eight rainfall events studied display a high probability (>90%) of falling within the second zone, besides the already noted exception of Event Six (EV6)—for which an M(V) curve could not be fitted—in addition to Event Eight (EV8), for which the first, second and third zones have low probabilities.

As we mentioned in previous section, we explored the relation between both a and b parameters with rainfall characteristics. Spearman correlation rank test outcomes are found in Tables 4 and 5.

The natural conclusion from these results is that the only hydrological variable significantly correlated to the total runoff volume V_{tot} ($\rho = 0.78$ and p-value = 0.02) and the total TSS mass M_{tot} ($\rho = 0.78$ and p-value = 0.02) is P. That is, the relationship between hydrographs and pollutographs (Fig. 4) confirms: TSS_{max} is positively correlated with Q_{max} ($\rho = 0.73$ with p-value = 0.04) and V_{tot} ($\rho = 0.79$ with p-value = 0.03). Likewise, there is positive correlation between V_{tot} and TSS_m ($\rho = 0.74$ with p-value = 0.05). Moreover, M_{tot} is highly correlated to Q_{max} ($\rho = 0.95$ with p-value < 0.01) and V_{tot} ($\rho = 0.98$ with p-value < 0.01), evincing that events with higher runoff flow rates present higher TSS concentrations.

Figs. 7 and 8 summarize the Spearman coefficient values and p-values, where the latter are expressed as –log (p-value).

Fig. 7 evidences the low correlation coefficients ($|\rho| < 0.75$) for hydrological variables and parameters a and b, while Fig. 8 evidences that Spearman correlation p-values are not significant (p-value > 0.05).

Ten thousand linear models were fitted for a and b M(V) curve parameters and hydrological event variables. Despite adjustment (adjusted $R^2 > 0.998$ for a and adjusted $R^2 > 0.876$ for b) and residual normality (p-values > 0.125 for both a and b per the Shapiro–Wilk normality test), most models exhibit insignificant b parameter coefficients (Fig. 9). Thus, PLS models are employed to assess the role of precipitation variables by taking into account the fitted PLS models' correspondent weights (β coefficients in Eq. (6)) for 10,000 simulations).

Figs. 10 and 11 include the PLS for hydrological variables, as well as a and b fitting parameters. These regressions help distinguish the relevance of hydrological variables for first flush—in other words, they handle uncertainties in M(V) relations. The variability of models obtained from PLS (10,000 total) is countered with Eqs. (7) and (8) to determine the confidence intervals associated with weight factors for a and b equations, respectively.

$$a = [0.86;\ 4.37] + [-0.05;\ 0.20]\mathrm{ADWP} + [-0.14;\ 0.51]P + [0.18;\ 0.64]I_m + [-0.30;\ -0.19]I_{max} + [-0.09;\ 0.29]D \quad (7)$$

$$b = [0.6679;\ 0.7759] + [-0.0029;\ -0.0003]\mathrm{ADWP} + [-0.0135;\ 0.0175]P + [-0.0767;\ -0.0320]I_m + [0.0146;\ 0.0316]I_{max} + [-0.0046;\ 0.0028]D \quad (8)$$

Figs. 10 and 11 allow one to infer: PLS models are more accurately adjustable for *a* than for *b*. Similarly, PLS models for parameter *a* appear to be more robust than those for *b*.

PLS models for both *a* and *b* parameters measure the importance of hydrological variables by computing the absolute values of the weighting factors (β_1–β_n, Eq. (6)). This procedure quantifies the effect of each hydrological variable on first flush, from Position 1 (most important) to 5 (least important). Undertaken for each of the 10,000 PLS models fitted, this step is combined with a RI to reveals the number of times (1 to 10,000) that a certain hydrological variable occupies the same position; subsequently, this number is divided by the total number of simulations (10,000) to arrive at the percentages displayed in Fig. 12. As Fig. 12 avers, I_{m}, and $I_{\max}$ are the hydrological variables most relevant to *a* and *b*.

4. Conclusions

In this paper we proposed a methodology that assesses the occurrence probability of first flush in a storm drain inlet. Data from a storm drain inlet located on a highly transited avenue in Bogota, Colombia over the course of October and November, 2011 ("rainy" months) were used to assay the methodology, referred to as OFFIS. OFFIS' design does not call for specific technological tools, which translates into applicability across a broad spectrum.

The analysis carried out on eight rainfall events (of which six ended with viable data) allow for the estimation of first flush probabilities. TSS concentrations reflect those reported in similar studies in terms of magnitude and situation, i.e. urban road runoff [2,28,29]. Significant correlations between hydrographs and pollutographs are established, suggesting that: (i) TSS discharge mitigation can be best achieved by way of focusing on points with the most runoff; (ii) TSS pollution assessment can be done in real or deferred time (i.e. after road runoff) using only hydraulic and/or hydrological information; (iii) rainfall-runoff model calibration can be done by means of filling out pollutographs for each event.

The Monte Carlo method resulted in high probabilities (greater than 90%) observed for medium TSS first flush—six of the eight events monitored. However, the Spearman correlation test fails to show significant correlations between the first flush phenomenon and the hydrological variables of each precipitation event. And although PLS analysis concludes that average and maximum rainfall intensities are the hydrological variables most relevant to first flush, this conclusion is premised upon uncertainties stemming from M(V) relations for the events. Verification of these results would demand first flush real-time control or even the inference of M(V) curves for non-sampled rainfall events based on hydrological information. Both situations only become possible with the monitoring of more rainfall events and by adjusting for uncertainties concomitant to the collection of hydrological data.

Even though water volume data and pollutant mass data were adjusted to the M(V) function proposed by Bertrand-Krajewski et al. [14], these data do not prove to be representative of the eight events. Therefore, it is advisable to seek alternative ways to characterize the first flush phenomenon, such as the power and polynomial functions found in Ma et al. [10].

References

[1] L. Lundy, J.B. Ellis, D.M. Revitt, Risk prioritisation of stormwater pollutant sources, Water Res. 46 (2012) 6589–6600, doi: 10.1016/j.watres.2011.10.039.

[2] M. Zhang, H. Chen, J. Wang, G. Pan, Rainwater utilization and storm pollution control based on urban runoff characterization, J. Environ. Sci. 22 (2010) 40–46.

[3] V. Novotný, G. Chesters, Handbook of Nonpoint Pollution: Sources and Management, Van Nostrand Reinhold, New York, NY, 1981.

[4] S. Artina, G. Bardasi, F. Borea, C. Franco, M. Maglionico, A. Paoletti, U. Sanfilippo, J. Ball, I. Joliffe, Water quality modelling in ephemeral streams receiving urban overflows, in: J. Ball, I. Joliffe (Eds.), The Pilot Study in Bologna, Sydney, Australia, 1999, pp. 1589–1596.

[5] J.-L. Bertrand-Krajewski, A model for solid production and transport for small urban catchments: Preliminary results 25 (1992) 29–35.

[6] L. Li, C. Yin, Q. He, L. Kong, Contribution of pollution load of storm runoff in urban areas of Hanyang, Wuhan City on the receiving water, China Environ. Sci. 27 (2007) 312–316.

[7] L. Li, C. Yin, Q. He, L. Kong, First flush of storm runoff pollution from an urban catchment in China, J. Environ. Sci. 19 (2007) 295–299, doi: 10.1016/S1001-0742(07)60048-5.

[8] A. Deletic, The first flush load of urban surface runoff, Water Res. 32 (1998) 2462–2470, doi: 10.1016/S0043-1354(97)00470-3.

[9] J.H. Lee, K.W. Bang, L.H. Ketchum Jr., J.S. Choe, M.J. Yu, First flush analysis of urban storm runoff, Sci. Total Environ. 293 (2002) 163–175, doi: 10.1016/S0048-9697(02)00006-2.

[10] Z.-B. Ma, H.-G. Ni, H. Zeng, J.-B. Wei, Function formula for first flush analysis in mixed watersheds: A comparison of power and polynomial methods, J. Hydrology 402 (2011) 333–339, doi: 10.1016/j.jhydrol.2011.03.029.

[11] J.M. Hathaway, R.S. Tucker, J.M. Spooner, W.F. Hunt, A traditional analysis of the first flush effect for nutrients in stormwater runoff from two small urban catchments, Water Air Soil Pollut. 223 (2012) 5903–5915, doi: 10.1007/s11270-012-1327-x.

[12] J. Im, K. Cho, K. Gil, Determination of the first-flush criteria from railway bridge area, Desalin. Water Treat. (2015) 1–15, doi: 10.1080/19443994.2014.997990.
[13] J. He, C. Valeo, A. Chu, N.F. Neumann, Characterizing physicochemical quality of storm-water runoff from an urban area in Calgary, Alberta, J. Environ. Eng. 136 (2010) 1206–1217, doi: 10.1061/(ASCE)EE.1943-7870.0000267.
[14] J.-L. Bertrand-Krajewski, G. Chebbo, A. Saget, Distribution of pollutant mass vs volume in stormwater discharges and the first flush phenomenon, Water Res. 32 (1998) 2341–2356, doi: 10.1016/S0043-1354(97)00420-X.
[15] R Core Team, R: A Language and Environment for Statistical Computing, R Foundation for Statistical Computing, Vienna, Austria, 2014. Available from: <http://www.R-project.org/>.
[16] E.W. Rice, L. Bridgewater, American Public Health Association, American Water Works Association, Water Environment Federation, Standard Methods for the Examination of Water and Wastewater, American Public Health Association, Washington, DC, 2012.
[17] International Organization for Standardization (ISO), Guide to the Expression of Uncertainty in Measurement, Geneva, Suiza, 1995.
[18] International Organization for Standardization (ISO), ISO/IEC Guide 98-3:2008 Incertitude de mesure—Partie 3: Guide pour l'expression de l'incertitude de mesure (Uncertainty of measurement - Part 3: Guide to the Expression of Uncertainty in Measurement) (GUM: 1995), first ed., Geneva, Suiza, 2008.
[19] NF ENV 13005, Guide pour l'expression de l'incertitude de mesure (Guide to the Expression of Uncertainty in Measurement), ANFOR, Paris, France, 1999.
[20] S.R. Poulter, Monte Carlo simulation in environmental risk as-sessment—Science, policy and legal issues, risk: Health, Saf. Environ. 9 (1998) 7–26.
[21] S. Greenland, Sensitivity analysis, Monte Carlo risk analysis, and Bayesian uncertainty assessment, Risk Anal. 21 (2001) 579–584, doi: 10.1111/0272-4332.214136.
[22] E.P. Smith, Uncertainty Analysis, in: Encyclopedia of Environmetrics, John Wiley & Sons, Ltd, 2006. Available from: <http://onlinelibrary.wiley.com/doi/10.1002/9780470057339.vau001.pub2/abstract> (accessed November 12, 2015).
[23] S. Sharifi, A. Massoudieh, M. Kayhanian, A stochastic stormwater quality volume-sizing method with first flush emphasis, Water Environ. Res. 83 (2011) 2025–2035, doi: 10.2175/106143011X12989211.
[24] B.-H. Mevik, R. Wehrens, The pls package: Principal component and partial least squares regression in R, J. Stat. Software 18 (2007) 1–24.
[25] J.M. Chambers, Linear models, in: J.M. Chambers, T.J. Hastie (Eds.), Statistical Models in S, Chapman & Hall/CRC, Boca Raton, Fla, 1992.
[26] A. Rada-Ariza, A. Torres, Preliminary Assessment of the Influence of Salitre Basin Rainfall on the Pumping Operation of Salitre Wastewater Treatment Plant (Bogota), Porto Alegre, Brazil, 2011, p. 8.
[27] Google Maps, Google Maps. (n.d.). Available from: <https://www.google.com/maps/place/Bogot%C3%A1,+Bogota,+Colombia/@4.6274385,-74.0658435,17z/data=!4m2!3m1!1s0x8e3f9bfd2da6cb29:0x239d635520a33914> (accessed May 19, 2014).
[28] M.C. Gromaire-Mertz, S. Garnaud, A. Gonzalez, G. Chebbo, Characterisation of urban runoff pollution in Paris, Water Sci. Technol. 39 (1999) 1–8, doi: 10.1016/S0273-1223(99)00002-5.
[29] I. Gnecco, C. Berretta, L.G. Lanza, P. La Barbera, Storm water pollution in the urban environment of Genoa, Italy, Atmos. Res. 77 (2005) 60–73, doi: 10.1016/j.atmosres.2004.10.017.
[30] J.W. Tukey, Exploratory Data Analysis, first ed., Pearson Reading, Massachusetts, 1977.